ISSN 0030-400X, Optics and Spectroscopy, 2013, Vol. 115, No. 4, pp. 499–507. © Pleiades Publishing, Ltd., 2013.
Original Russian Text © L.A. Nesterov, S.V. Fedorov, N.N. Rosanov, B.N. Levinsky, B.D. Fainberg, 2013, published in Optika i Spektroskopiya, 2013, Vol. 115, No. 4, pp. 572–580.

CONDENSED-MATTER SPECTROSCOPY

Analysis of Bistability in Molecular *J* Aggregates under Their Resonant Optical Excitation Taking into Account Multiparticle Effects

L. A. Nesterov[a, b], S. V. Fedorov[a, b], N. N. Rosanov[a, b, c], B. N. Levinsky[d], and B. D. Fainberg[d, e]

[a] *St. Petersburg National Research University of Information Technologies, Mechanics, and Optics, St. Petersburg, 197101 Russia*

[b] *Vavilov State Optical Institute, St. Petersburg, 199034 Russia*

[c] *Ioffe Physical-Technical Institute, Russian Academy of Sciences, St. Petersburg, 194021 Russia*

[d] *Holon Institute of Technology, 58102 Holon, Israel*

[e] *School of Chemistry, Tel Aviv University, 69978 Tel Aviv, Israel*

e-mail: nrosanov@yahoo.com, fainberg@hit.ac.il

Received March 25, 2013

Abstract—Using a model of a homogeneous chain of molecules, we have analyzed bistability in resonantly excited *J* aggregates taking into account three-particle contributions to the exciton–exciton annihilation. These contributions, which have an interference nature, have previously been calculated in a work by B.N. Levinsky, L.A. Nesterov, B.D. Fainberg, and N.N. Rosanov (Opt. Spectrosc. **115** (3), 406 (2013)) in the course of derivation of equations of motion for *J* aggregates from first principles. Factorization of expectation values that correspond to these contributions leads to a closed system of equations in which not only pair, but also triple, interactions between molecules of the chain are taken into account. Numerical calculations have been performed, and their results have been compared with those obtained in calculations without taking into account three-particle contributions. We have shown that, on the whole, the inclusion of three-particle interference contributions in equations of motion leads to a restriction of the domain of existence of hysteresis. This, in turn, makes it possible to more reliably single out a real range of parameters in which nonlinear optical effects can considerably manifest themselves.

DOI: 10.1134/S0030400X13100135

1. INTRODUCTION

Excitation of *J* aggregates by resonant radiation can give rise to nonlinear effects in these systems. Thus, in [1, 2], an effect of bistability in a single *J* aggregate has been predicted theoretically, and, in [3–5], this effect was predicted in an ensemble of molecular aggregates in a thin film. The mechanisms by which bistability arises in one molecular aggregate and in an ensemble of molecular aggregates are different (their detailed comparison can be found in [4]). In theoretical study [6], the possibility of excitation of a dissipative soliton in an individual *J* aggregate was demonstrated in terms of a model of three-level molecules. In this latter case, a traditional system of equations was investigated, which was obtained based on a semiclassical approach. In these equations, only two-particle interactions are taken into account usually in the factorized form. An analysis of these equations from the first principles showed that three-particle contributions also arise in them, which are caused by the exciton–exciton annihilation effect [7]. A closed system of equations that takes into account the three-particle interaction can be obtained by neglecting completely correlations between molecules and factorizing the expectation values that correspond to these three-particle contributions. The system of equations obtained in this way is the simplest example of taking into account multiparticle effects related to two-exciton annihilation.

It should be kept in mind that three-particle contributions obtained in this way have an essentially interference nature. Indeed, characteristic interference phenomena occur when the transition probability amplitude from a given initial to a given final state is a sum of two or more partial amplitudes, which have rather well-determined phase states. Thus, e.g., the quantity

$$\Gamma_{pmmk} = \frac{2\pi}{\hbar}\sum_{\nu} V_{pm}V_{mk}\delta(E_{f\nu} - 2E_e), \quad p \neq k,$$

(decay constant from formula (58) in [7]) is related to interference of different pathways of decay of the two-exciton state with participation of molecule m. This state can decay because of the interaction either with molecule p (V_{pm}) or with molecule k (V_{mk}), and it is impossible to know which of the pathways is, in fact, realized.

Analysis shows that factorized three-particle contributions can include as a multiplier an expectation value of the operator of the number of molecules at the lowest level. A particular feature of the considered systems [1, 2, 6] is that, in the equilibrium state, this expectation is close to unity, because the probability of population of upper levels of molecules is small. This immediately follows from the normalization condition that is accepted in this work [7],

$$N_{mg} + N_{me} + N_{mf} = 1,$$

in which N_{mg}, N_{me}, and N_{mf} are the operators of the number of molecules at site m at the first, second, and third levels, respectively. Therefore, the above three-particle contributions are, in fact, two-particle ones and coincide on the order of magnitude with two-particle contributions that appear in the traditional system of equations. Therefore, even this circumstance alone can quantitatively and qualitatively affect the properties of objects under study. Below, taking into account new contributions to equations of motion, we analyze the bistability in J aggregates in a special case that corresponds to the model of a homogeneous chain of molecules. This model assumes that the individual characteristics of all molecules do not depend on their place in the chain. Numerical calculations are performed, and their results are compared with the results obtained in [6].

2. MODIFIED SYSTEM OF EQUATIONS OF MOTION FOR ONE-PARTICLE EXPECTATION VALUES

In this section, we consider a modified system of equations from [6], in which we additionally take into account multiparticle contributions due to the exciton–exciton annihilation mechanism. The system of equations from [6] is a closed system of equations for one-particle density matrices, which describe the behavior of different molecules in the J aggregate. In order to obtain a modified system of equations, we will use formulas (38) and (39), as well as (60)–(62), from [7]. All the three-particle expectation values in the three latter equations are those that represent multiparticle contributions, which will be taken into account in these calculations for the first time. We should note, as well, that the two-particle expectation values $\langle b_n N_{le}\rangle$ in Eq. (62) from [7] also arose from three-particle contributions of the type $\langle N_{le} N_{mg} b_n\rangle$ after the substitution of the equality $N_{mg} = 1 - N_{me} - N_{mf}$ into them (see (1) from [7]) and are also taken into account in calculations for the first time. It should be noted that the contribution from N_{mf} is usually neglected because of a rapid decay of the third level.

To obtain a closed system of the equations listed above, it is necessary to factorize all multiparticle expectation values that appear in these equations. Let us perform this factorization and, for convenience of comparison with the preceding results, let us write the obtained system of equations in terms of one-particle density matrices as was done in [6]. It can be easily shown that

$$\langle N_{kf}\rangle = \rho_{33}^{(k)}, \quad \langle N_{ke}\rangle = \rho_{22}^{(k)},$$
$$\langle N_{kg}\rangle = \rho_{11}^{(k)}, \quad \langle b_k\rangle = R_k/2, \quad w = 2\alpha_s.$$

As a result, we arrive at the following system of equations:

$$\begin{aligned}\dot\rho_{11}^{(k)} &= \frac{1}{2}\mathrm{Re}\left[\sum_{l=1}^{N}(\gamma_{lk} + i\Delta_{lk})R_l R_k^* - i\Omega R_k^*\right]\\ &+ \Gamma_{31}\rho_{33}^{(k)} + \Gamma_{21}\rho_{22}^{(k)} + \alpha_s\rho_{22}^{(k)}\left[\rho_{22}^{(k-1)} + \rho_{22}^{(k+1)}\right]\\ &+ \frac{1}{4}\alpha_s\,\mathrm{Re}\left[R_k\left(R_{k-2}^*\rho_{22}^{(k-1)} + R_{k+2}^*\rho_{22}^{(k+1)}\right)\right],\end{aligned} \tag{1}$$

$$\begin{aligned}\dot\rho_{22}^{(k)} &= -\frac{1}{2}\mathrm{Re}\left[\sum_{l=1}^{N}(\gamma_{lk} + i\Delta_{lk})R_l R_k^* - i\Omega R_k^*\right]\\ &+ \Gamma_{32}\rho_{33}^{(k)} - \Gamma_{21}\rho_{22}^{(k)} - 2\alpha_s\rho_{22}^{(k)}\left[\rho_{22}^{(k-1)} + \rho_{22}^{(k+1)}\right]\\ &- \frac{1}{4}\alpha_s\,\mathrm{Re}\left[R_k\left(R_{k-2}^*\rho_{22}^{(k-1)} + R_{k+2}^*\rho_{22}^{(k+1)}\right)\right]\\ &- \frac{1}{4}\alpha_s\rho_{22}^{(k)}\left(R_{k-1}^*R_{k+1} + R_{k+1}^*R_{k-1}\right),\end{aligned} \tag{2}$$

$$\begin{aligned}\dot\rho_{33}^{(k)} &= -(\Gamma_{31} + \Gamma_{32})\rho_{33}^{(k)} + \alpha_s\rho_{22}^{(k)}\left[\rho_{22}^{(k-1)} + \rho_{22}^{(k+1)}\right]\\ &+ \frac{1}{4}\alpha_s\rho_{22}^{(k)}\left(R_{k-1}^*R_{k+1} + R_{k+1}^*R_{k-1}\right),\end{aligned} \tag{3}$$

$$\begin{aligned}\dot R_k &= -(\Gamma_\perp + i\Delta_k)R_k + \sum_{l=1}^{N}(\gamma_{lk} + i\Delta_{lk})R_l\left[\rho_{22}^{(k)} - \rho_{11}^{(k)}\right]\\ &- i\Omega\left[\rho_{22}^{(k)} - \rho_{11}^{(k)}\right] - \alpha_s R_k\left[\rho_{22}^{(k-1)} + \rho_{22}^{(k+1)}\right]\\ &- \frac{1}{2}\alpha_s\left(R_{k-2}\rho_{22}^{(k-1)} + R_{k+2}\rho_{22}^{(k+1)}\right)\left(1 - 2\rho_{22}^{(k)} - \rho_{33}^{(k)}\right)\\ &- \frac{1}{8}\alpha_s R_k\left(R_{k-1}^*R_{k+1} + R_{k+1}^*R_{k-1}\right).\end{aligned} \tag{4}$$

Here, dots above quantities in the left-hand sides of equations denote time derivatives. The diagonal elements of the density matrix are proportional to the populations of corresponding levels. Due to the normalization

$$\rho_{11}^{(k)} + \rho_{22}^{(k)} + \rho_{33}^{(k)} = 1 \tag{5}$$

we can eliminate quantities $\rho_{11}^{(k)}$ from (1). The diagonal elements of matrices γ_{lk} and Δ_{lk} obey the condition

$$\gamma_{ll} = 0, \quad \Delta_{ll} = 0, \tag{6}$$

while their off-diagonal elements are defined as

$$\gamma_{lk} = \frac{\mu^2}{\hbar a^3}\left\{\left[k_0 a\frac{\cos(k_0 a|l-k|)}{|l-k|^2} - \frac{\sin(k_0 a|l-k|)}{|l-k|^3}\right]\right.$$
$$\left.\times(1-3\cos^2\theta) + (k_0 a)^2\frac{\sin(k_0 a|l-k|)}{|l-k|}\sin^2\theta\right\},$$
$$\Delta_{lk} = \frac{\mu^2}{\hbar a^3}\left\{\left[\frac{\cos(k_0 a|l-k|)}{|l-k|^3} + k_0 a\frac{\sin(k_0 a|l-k|)}{|l-k|^2}\right]\right. \quad (7)$$
$$\left.\times(1-3\cos^2\theta) - (k_0 a)^2\frac{\cos(k_0 a|l-k|)}{|l-k|}\sin^2\theta\right\}.$$

In (4), the frequency detuning for the kth molecule appears,

$$\Delta_k = \omega_{21}^{(k)} - \omega_0 = \Delta_0 + \delta\Delta_k, \quad (8)$$

where $\omega_{21}^{(k)}$ is the frequency of transition $1 \to 2$ of the molecule at site k, ω_0 is the frequency of pumping, $k_0 = \omega_0/c$, Δ_0 is the average value of the detuning for molecules in the chain, and $\delta\Delta_k$ is its statistical straggling with the zero average value and specified variance (for each molecule with number k, this quantity is treated irrespective of its values for other molecules). Quantity $\Omega = \mu E_1/\hbar$ is the Rabi frequency, which is proportional to the amplitude of the external field

$$E = E_1(t)\exp(-i\omega_0 t). \quad (9)$$

Other parameters of the problem are the matrix element of dipole moment μ for the transition $1 \to 2$, angle θ between the dipole moment and the axis of the chain, relaxation constants Γ_{ik} and $\Gamma_\perp$, exciton–exciton annihilation parameter α_s, and constant a of the one-dimensional lattice of molecules. Comparing these notations with those from [7], we can see that $\Gamma_{21} = \gamma_2$ and $\Gamma_\perp = \gamma_\perp$.

3. DIMENSIONLESS FORM OF EQUATIONS OF MOTION

For further calculations, we will use normalized system of equations (1)–(4). This normalization can be done in different ways; however, one of the most convenient of them is related to the normalization to parameters that arise naturally in terms of homogeneous regimes. For these regimes, $\rho_{lm}^{(k)} \approx \rho_{lm}$ and the parameters of all molecules are considered as identical averaged quantities. Below, all hysteresis effects will be investigated precisely for these regimes.

It will shown further that, in the case of homogeneous regimes, two natural parameters arise,

$$\gamma_R = 2\sum_{l-k=1}^{N/2}\gamma_{lk}, \quad \Delta_L = 2\sum_{l-k=1}^{N/2}\Delta_{lk}, \quad (10)$$

which are collective contributions of surrounding molecules to the decay and shift of the second level of the individual molecule. For J aggregates, $\Delta_L < 0$, $|\Delta_L| \gg \gamma_R$, and the typical scatter of frequency detunings is $(0.1–0.2)|\Delta_L|$. Analysis showed that it is convenient to normalize the time and all the parameters of the system using the quantity γ_R. In what follows, all the coefficients of Eqs. (1)–(4) normalized to γ_R will be denoted by symbols with bars. However, the normalized constant α_S will be denoted as α. We also note that, for the normalized time, its previous designation will be retained. Thus,

$$\gamma_R t \to t, \quad A/\gamma_R = \bar{A}, \quad \alpha_S/\gamma_R = \alpha, \quad (11)$$

where A is an arbitrary coefficient of system (1)–(4).

In calculations, we used dimensionless equations for diagonal elements of the density matrix that correspond to the upper, $\rho_3(k,i) = \rho_{33}^{(k)}(i)$, and intermediate, $\rho_2(k,i) = \rho_{22}^{(k)}(i)$, levels, as well as for off-diagonal elements $R(k,i) \equiv R_k(i)$. Here, k is the number of the molecule in the linear chain and i is the number of the chain with a different distribution of frequency detunings $\Delta_k(i)$ (8) of individual molecules. Below, for brevity, index i is omitted, but, of course, is implied.

The dynamic model is reduced to solving a set of uncoupled equations for different chains with respect to dimensionless time t. Designating $\mathbf{R} = \{R_k(i), k = 1, \ldots, N\}$, we have

$$\frac{d}{dt}\rho_3(k) = -\bar{\Gamma}\rho_3(k) + \alpha\rho_2(k)[\rho_2(k-1) + \rho_2(k+1)] + \frac{1}{2}\alpha\rho_2(k)\,\mathrm{Re}(R_{k-1}^* R_{k+1}), \quad (12)$$

$$\frac{d}{dt}\rho_2(k) = -\frac{1}{2}|R_k|^2 - \frac{1}{2}\mathrm{Re}\,R_k^*[(\delta\hat{\bar{g}}\mathbf{R})_k - i\bar{\Omega}] + \bar{\Gamma}_{32}\rho_3(k) - \bar{\Gamma}_{21}\rho_2(k) - 2\alpha\rho_2(k)[\rho_2(k-1) + \rho_2(k+1)] - \frac{1}{4}\alpha\,\mathrm{Re}[R_k(R_{k-2}^*\rho_2(k-1) + R_{k+2}^*\rho_2(k+1))] - \frac{1}{2}\alpha\rho_2(k)\,\mathrm{Re}(R_{k-1}^* R_{k+1}), \quad (13)$$

$$\frac{d}{dt}R_k + (\bar{\gamma} + i\bar{\Delta}(k))R_k = i\bar{\Omega} - (\delta\hat{\bar{g}}\mathbf{R})_k + (1 + i\bar{\Delta}_L)R_k\rho_d(k) + [(\delta\hat{\bar{g}}\mathbf{R})_k - i\bar{\Omega}]\rho_d(k) - \alpha R_k[\rho_2(k-1) + \rho_2(k+1)] - \frac{1}{2}\alpha[R_{k-2}\rho_2(k-1) + R_{k+2}\rho_2(k+1)][1 - \rho_d(k)] \quad (14)$$

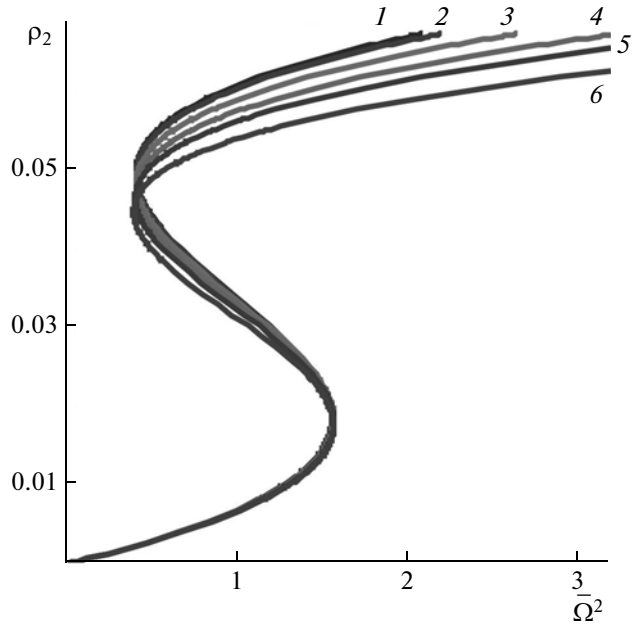

Fig. 1. Hysteresis for the population of the second excited level upon variation of the Rabi frequency according to formula (20). The coefficient of the exciton–exciton annihilation acquires values α = (*1*) 0, (*2*) 1, (*3*) 5, (*4*) 10, (*5*) 15, and (*6*) 25; $\bar{\Delta} = -10$.

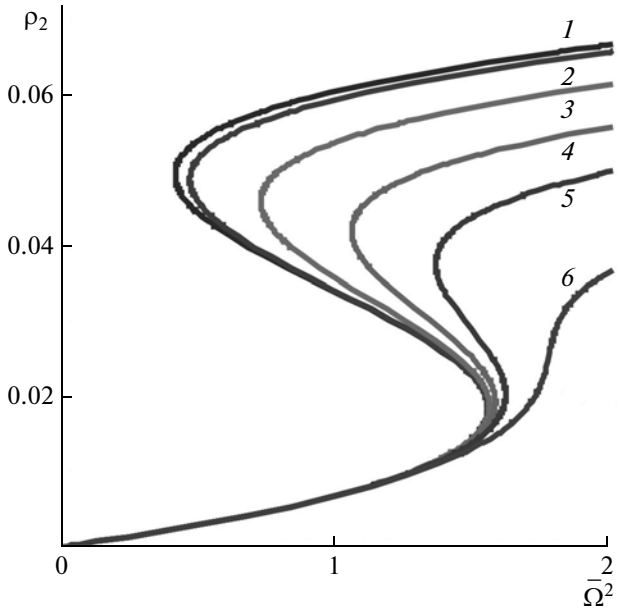

Fig. 2. Hysteresis for the population of the second excited level ρ_2 upon variation of the Rabi frequency for the stationary solution of Eqs. (17)–(19): α = (*1*) 0, (*2*) 1, (*3*) 5, (*4*) 10, (*5*) 15, and (*6*) 25. Hysteresis vanishes at a value of the exciton–exciton annihilation constant $\alpha \approx 22.7$.

$$-\frac{1}{4}\alpha R_k \,\mathrm{Re}(R^*_{k-1}R_{k+1}),$$

where

$$\rho_d(k) = 1 - \rho_1 + \rho_2 = 2\rho_2 + \rho_3,$$

$$\mathrm{Re}\, R^*_k(\hat{\bar{g}}\mathbf{R})_k = \mathrm{Re}\, R^*_k(\delta\hat{\bar{g}}\mathbf{R})_k + |R_k|^2.$$

Here, the following notation is used:

$$\begin{gathered}\hat{\bar{g}} = \{\bar{g}_{kl}\}, \quad \bar{g}_{kl} = \bar{\gamma}_{kl} + i\bar{\Delta}_{kl},\\ \delta\hat{\bar{g}} = \{\delta\bar{g}_{kl}\}, \quad \delta\bar{g}_{kl} = \bar{g}_{kl} - (1 + i\bar{\Delta}_L)\delta_{kl},\\ \bar{\gamma} = 1 + \bar{\Gamma}_\perp, \quad \bar{\Delta} = \bar{\Delta}_0 + \bar{\Delta}_L,\\ \bar{\Delta}(k) = \bar{\Delta} + \delta\Delta_k(i).\end{gathered} \tag{15}$$

4. THE MODEL OF A HOMOGENEOUS CHAIN; FORM OF EQUATIONS

For the homogeneous regimes (the same state of all molecules), we do not consider the boundary conditions at the ends of the chain of molecules, i.e., proceed to the limit $N \to \infty$. Let us write Eqs. (12)–(14) for the elements of the density matrix of one chain,

$$\rho_{2,3}(k,i,t) = \rho_{2,3}(t), \quad R(k,i,t) = R(t), \quad \bar{\Delta}(k) = \bar{\Delta},$$

which do not depend on the number of the molecule.We will also take into account that, in the limit $N \to \infty$, parameter γ_R changes to

$$\gamma_R|_{N\to\infty} = 2\sum_{l-k=1}^{\infty}\gamma_{lk}. \tag{16}$$

As a result, for an infinite homogeneous chain, we have the following system of equations:

$$\begin{aligned}\frac{d}{dt}\rho_2(t) = &-\frac{1}{2}|R(t)|^2 + \frac{1}{2}\bar{\Omega}\,\mathrm{Im}\,R(t) + \bar{\Gamma}_{32}\rho_3(t)\\ &-\bar{\Gamma}_{21}\rho_2(t) - 4\alpha\rho_2^2(t) - \alpha|R(t)|^2\rho_2(t),\end{aligned} \tag{17}$$

$$\frac{d}{dt}\rho_3(t) = -\bar{\Gamma}\rho_3(t) + 2\alpha\rho_2^2(t) + \frac{1}{2}\alpha|R(t)|^2\rho_2(t), \tag{18}$$

$$\begin{aligned}\frac{d}{dt}R(t) + [\bar{\gamma} + i\bar{\Delta}]R(t) = &(1 + i\bar{\Delta}_L)\rho_d(t)R(t)\\ &+ i\bar{\Omega}[1 - \rho_d(t)] - 2\alpha\rho_2(t)R(t)\\ -\alpha\rho_2(t)R(t)[1 - \rho_d(t)] &- \frac{1}{4}\alpha R(t)|R(t)|^2.\end{aligned} \tag{19}$$

Analysis of this system shows that, in the approach used in this work, an additional relaxation channel, which is related to taking into account new contributions, can lead, in particular, to a more efficient decay of the second excited level of molecules of the chain.

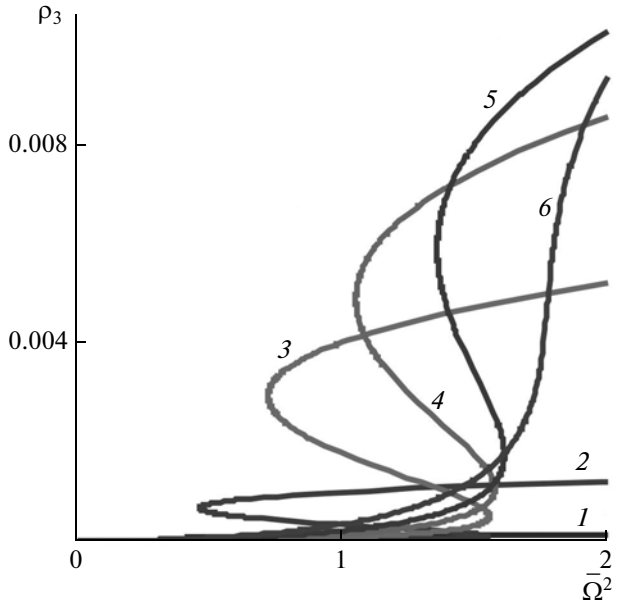

Fig. 3. Hysteresis for the population of the third level ρ_3 upon variation of the Rabi frequency: $\alpha = (1)$ 0, (2) 1, (3) 5, (4) 10, (5) 15, and (6) 25. Hysteresis vanishes at $\alpha \approx 22.7$.

The manifestation of the bistability is related to the hysteresis dependence of the parameters of the system under consideration on the intensity of the incident radiation or, in our case, on squared Rabi frequency $\bar{\Omega}^2$. In the general case, this dependence can arise at a fixed value of $\bar{\Omega}$ and on other quantities that characterize the system, e.g., on normalized detuning $\bar{\Delta}$. In order to investigate these hysteresis dependences, it is necessary to consider stationary regimes for system of equations (17)–(19) by zeroing their time derivatives. We have to emphasize that, here, we are not investigating the stability of these regimes. This issue will be the subject of an independent investigation.

In order to have the possibility of comparing new results with results of [6], we will initially consider and analyze the hysteresis function from that work. In terms of dimensionless variables, this hysteresis function will have the following form:

$$\frac{1}{2}\bar{\Omega}^2 = \frac{\bar{\Gamma}_{21}\rho_2 + 2\alpha\rho_2^2(2\bar{\Gamma} - \bar{\Gamma}_{32})/\bar{\Gamma}}{(1-\rho_d)(\bar{\Gamma}_\perp + 2\alpha\rho_2)} \times [(\bar{\gamma} - \rho_d + 2\alpha\rho_2)^2 + (\bar{\Delta} - \bar{\Delta}_L\rho_d)^2]. \quad (20)$$

In particular, for $\alpha = 0$, we have

$$\frac{1}{2}\bar{\Omega}^2 = \frac{\bar{\Gamma}_{21}\rho_2}{(1-2\rho_2)\bar{\Gamma}_\perp}\left[(\bar{\gamma} - 2\rho_2)^2 + (\bar{\Delta} - 2\bar{\Delta}_L\rho_2)^2\right]. \quad (21)$$

We consider the case of a chain of molecules with $N \to \infty$ and $k_0 a \ll 1$. It can be easily shown that, in this limit, $|\bar{\Delta}_L| \sim 1/(k_0 a)^3$ and, consequently, $|\bar{\Delta}_L| \gg 1$.

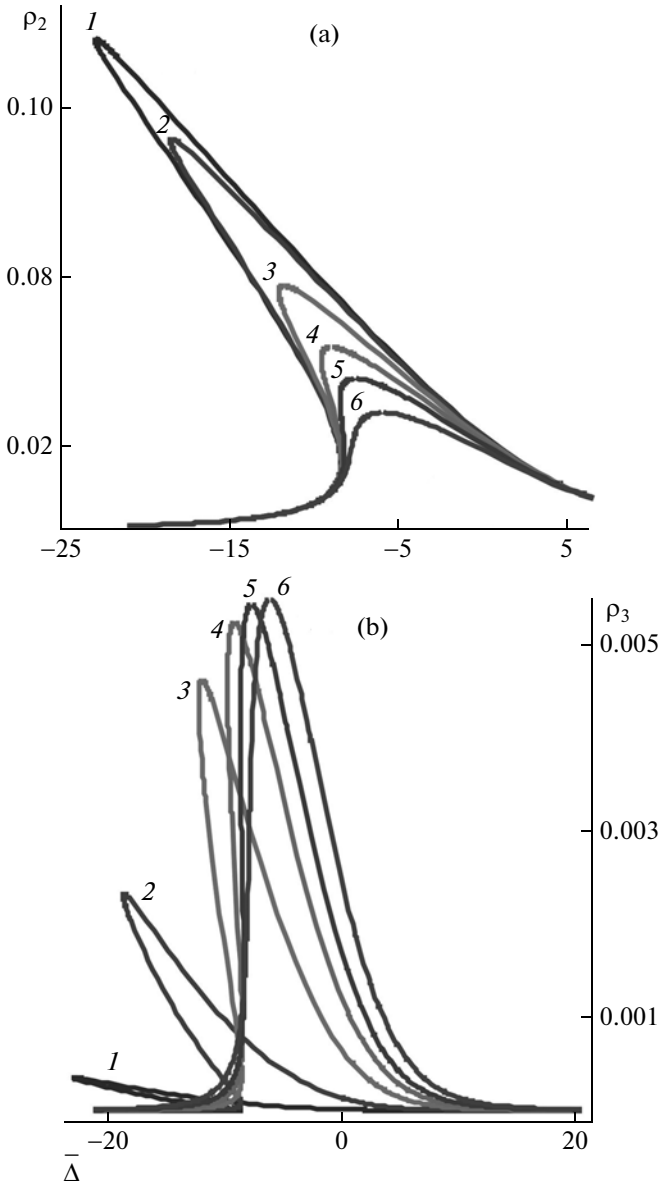

Fig. 4. Hysteresis for the populations of the (a) second and (b) third levels (ρ_2 and ρ_3, respectively) upon variation of the frequency detuning of the maintaining radiation $\bar{\Delta}$; $\bar{\Omega} = 1$; $\alpha = (1)$ 0, (2) 1, (3) 5, (4) 10, (5) 15, and (6) 25. Hysteresis vanishes at $\alpha \approx 15$..

At equilibrium, the populations of upper levels in *J* aggregates are small compared to lower levels. Assuming that $\rho_2 \ll 1$ and changing the variables

$$\rho_2 = r/2|\bar{\Delta}_L|, \quad \bar{\Omega} = \bar{\Omega}_s\sqrt{\bar{\Gamma}_{21}/\bar{\Gamma}_\perp\bar{\Delta}_L}, \quad (22)$$

we can approximately obtain

$$\bar{\Omega}_s^2 = r\left[\bar{\gamma}^2 + (\bar{\Delta} - sr)^2\right], \quad (23)$$

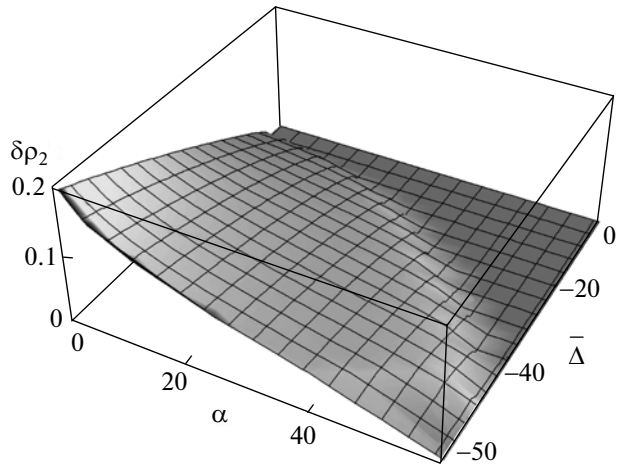

Fig. 5. Dependence of the hysteresis width of the population of the second level $\delta\rho_2 = \rho_{2,up} - \rho_{2,dn}$, where $\rho_{2,up}$ and $\rho_{2,dn}$ are the values of the left and right boundaries of the hysteresis in Fig. 2, on exciton–exciton annihilation coefficient α and detuning $\bar{\Delta}$.

where $s = \bar{\Delta}_L/|\bar{\Delta}_L|$ is the sign of the detuning. Equating $d\bar{\Omega}_s^2/dr$ to zero, one can easily find the roots of this equation,

$$r_{1,2} = \left(2\bar{\Delta}s \pm \sqrt{\bar{\Delta}^2 - 3\bar{\gamma}^2}\right)/3 \qquad (24)$$

and, therefore, determine the condition of existence of hysteresis at $\alpha = 0$,

$$|\bar{\Delta}| > \bar{\gamma}\sqrt{3}. \qquad (25)$$

Figure 1 shows curves of the hysteresis dependence of ρ_2 on $\bar{\Omega}^2$ that correspond to function (20) at $\bar{\Delta} = -10$ and $\alpha = 0$, 1, 5, 10, 15, and 25. In this case, the values of all the remaining parameters that were used in these calculations and for plots that will be further presented in this work are as follows: $k_0 a = 0.1$, $\sin^2\Theta = 1/3$, $\bar{\Gamma}_{31} = 0.1$, $\bar{\Gamma}_{32} = 10$, $\bar{\Gamma}_{21} = 1$, $\bar{\Delta}_L = -98.8$, $\bar{\gamma} = 2.1$, and $\bar{\Gamma}_\perp = 1.1$. On the one hand, the choice of these parameters is oriented to the results of [6] and, in part, of [1, 2], and, on the other hand, it is related to the necessity of taking into account to a greater degree the rapidity of depopulation of the third level, especially upon calculation of multiparticle effects.

From Fig. 1, it follows that the hysteresis exists in a rather wide range of values $\alpha \geq 0$. More detailed calculations show that the range of existence of the hysteresis with respect to this parameter and at $\bar{\Delta} = -10$ reaches a value of $\alpha \approx 40$. However, the analysis given below shows that taking into account multiparticle interference contributions leads to an almost twofold decrease in the dimension of this range.

5. HYSTERESIS UPON TAKING INTO ACCOUNT MULTIPARTICLE EFFECTS

Let us now consider hysteresis dependences that arise when multiparticle contributions are taken into account. By analyzing stationary regimes for Eqs. (17)–(19), we can obtain an analog of Eq. (20), but, however, in a considerably more complicated form,

$$\frac{1}{2}\bar{\Omega}^2 = \frac{[\bar{\Gamma}_{21}\rho_2 + 2\alpha(2 - \bar{\Gamma}_{32}/\bar{\Gamma})\rho_2^2](A^2 + B^2)}{(\rho_1 - \rho_2)\delta A}. \qquad (26)$$

Here,

$$\begin{aligned}(\rho_1 - \rho_2) &= 1 - 2\rho_2 - 2(\alpha/\bar{\Gamma})\rho_2^2 - (\alpha/\bar{\Gamma})|R|^2\rho_2/2,\\ A &= \bar{\Gamma}_\perp + 2\alpha\rho_2 + (1 + \alpha\rho_2)(\rho_1 - \rho_2) + \alpha|R|^2/4,\\ \delta A &= A - [1 + \alpha\rho_2(2 - \bar{\Gamma}_{32}/\bar{\Gamma})](\rho_1 - \rho_2) \qquad (27)\\ &= \bar{\Gamma}_\perp + 2\alpha\rho_2 - \alpha(1 - \bar{\Gamma}_{32}/\bar{\Gamma})\rho_2(\rho_1 - \rho_2) + \alpha|R|^2/4,\\ B &= \bar{\Delta}_0 + \bar{\Delta}_L(\rho_1 - \rho_2).\end{aligned}$$

Therefore, expressions (27) contain not only the dependence on ρ_2 but also the dependence on $|R|^2$. In turn, the performed analysis showed that, for $|R|^2$, a quadratic equation can be obtained, the coefficients of which depend only on ρ_2. By taking the positively defined root of this equation and substituting it into (27), we obtain a dependence of $\bar{\Omega}^2$ only on ρ_2. Because this solution can be further analyzed only numerically, we will not present it here explicitly, since it is too cumbersome.

Figure 2 presents hysteresis dependences of the population of the second level ρ_2 on $\bar{\Omega}^2$, which correspond to expression (26), at $\bar{\Delta} = -10$ and different values of the parameter α. It follows from the calculations that, with increasing α, the ranges of hysteresis contract, and hysteresis vanishes at a finite value $\alpha \approx 22.7$. Therefore, taking into account multiparticle contributions leads to an extremely substantial restriction (Section 4) of the range of existence of hysteresis as a function of the exciton–exciton annihilation constant. The same conclusions are obtained from analysis of Fig. 3, which shows hysteresis dependences of ρ_3 on the squared Rabi frequency.

Figure 4 shows hysteresis dependences of all the lowest quantities above on detuning $\bar{\Delta}$ at a fixed value of Rabi frequency $\bar{\Omega} = 1$ and the same values of α as above. It follows from these calculations that the hysteresis dependences vanish at $\alpha \approx 15$.

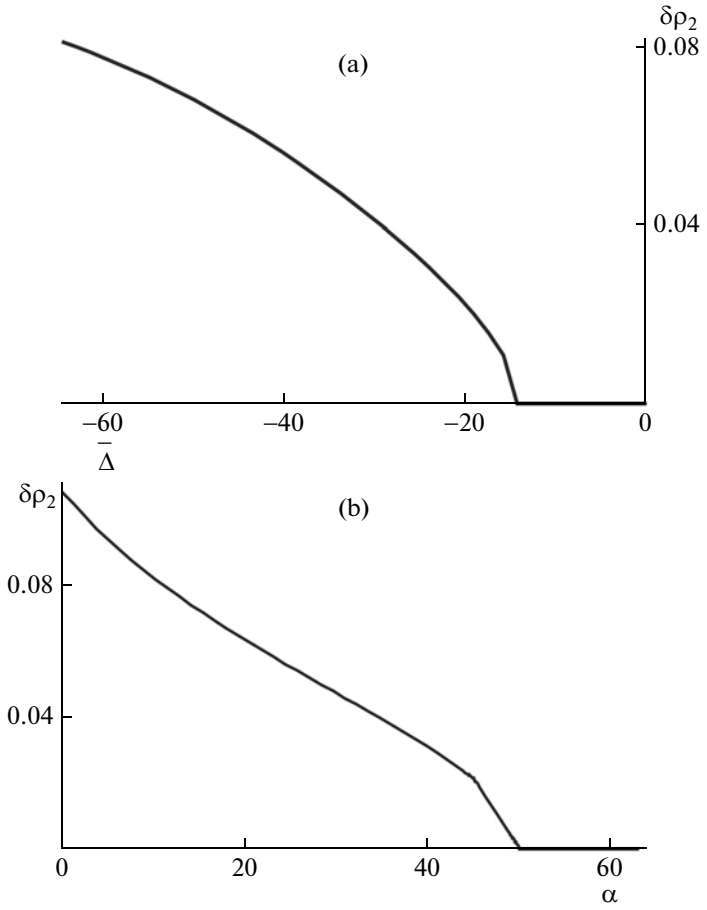

Fig. 6. Dependence of the hysteresis width of the population of the second level $\delta\rho_2 = \rho_{2,up} - \rho_{2,dn}$ (a) on detuning $\bar{\Delta}$ at $\alpha = 30$ and (b) on exciton–exciton annihilation coefficient α at $\bar{\Delta} = -34$. The range of existence of the hysteresis is limited for both parameters.

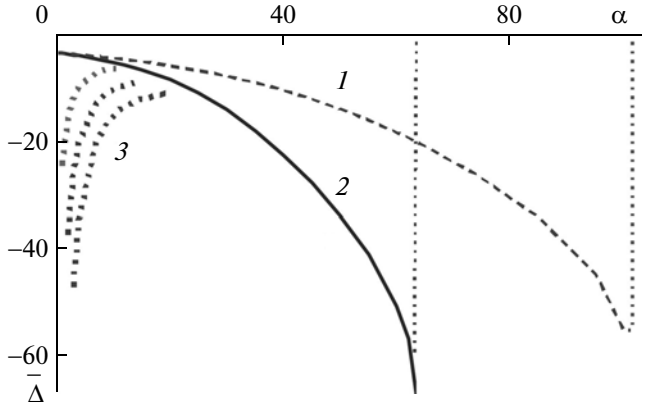

Fig. 7. Boundaries of the ranges of hysteresis existence in the plane of the parameters α and $\bar{\Delta}$. Curve *1* (dashed curve) bounds from above the hysteresis range described by formula (20). Boundary *2* (solid curve) corresponds to the case of taking into account multiparticle corrections. Set *3* of curves (from left to right) $\rho_3/\rho_2 = 0.1$, 0.2, and 0.3 corresponds to this case. Vertical dotted lines are boundaries with respect to the PMT α upon tending to which $|d\bar{\Delta}/d\alpha| \to \infty$.

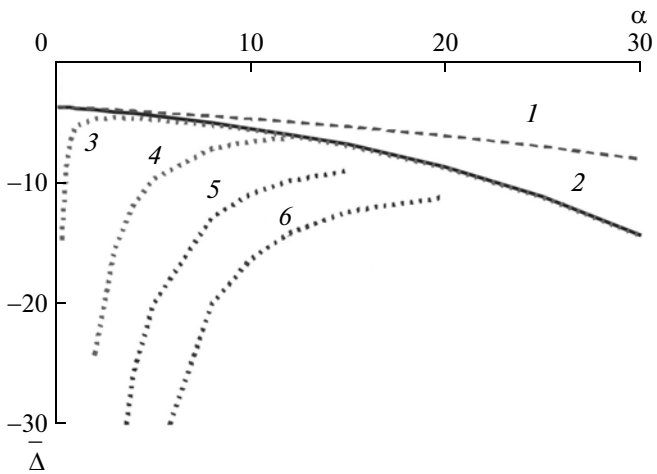

Fig. 8. Enlarged image of a part of Fig. 7 with additional curve *3* plotted at $\rho_3/\rho_2 = 0.01$; remaining curves are at $\rho_3/\rho_2 =$ (*4*) 0.1, (*5*) 0.2, and (*6*) 0.3.

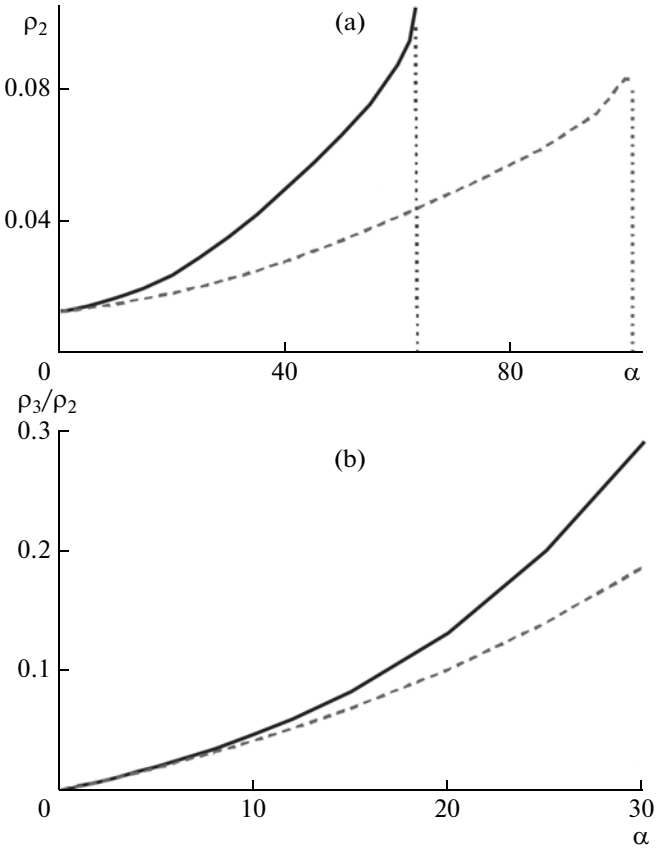

Fig. 9. (a) Dependence of ρ_2 on α at the boundaries of the ranges of existence of hysteresis: dashed curve corresponds to boundary *1* and solid curve corresponds to boundary *2* in Fig. 7. (b) Dependences of ρ_3/ρ_2 on α are plotted on the same boundaries and by the same curves.

Figure 5 shows the dependence of width of hysteresis $\delta\rho_2$ (difference between the right and left boundaries of hysteresis in Fig. 2) for the population of the second level on the detuning and exciton–exciton annihilation constant. The surface obtained makes it possible to determine not only the domain of existence of the hysteresis itself, but also, in principle, the most probable range of parameters in which a dissipative soliton can be formed. The intersection of this surface with the plane $\delta\rho_2 = 0$ evidently determines the boundary of the existence of the hysteresis.

In Fig. 6, curves of intersection of this surface by plane $\alpha = 30$, as well as $\bar{\Delta} = -34$, are shown. The obtained curves clearly show the refined boundaries of the existence of the hysteresis. These boundaries are shown in Fig. 7 in the plane of parameters α and $\bar{\Delta}$. Here, curve *1* bounds from above the range of hysteresis that corresponds to formula (20), while curve *2* does the same with respect to formula (26) for the case of taking into account multiparticle contributions. Vertical dotted lines correspond to values of α at which $|d\bar{\Delta}/d\alpha| \to \infty$. According to the calculations, these values are $\alpha \cong 63.4$ and $\alpha \cong 101.5$. Therefore, the plots clearly show that, upon taking into account multiparticle contributions, the range of existence of hysteresis considerably narrows, and, with respect to the parameter α, it decreases almost by 40%. Consequently, taking into account multiparticle contributions can, in principle, lead to an appreciable decrease in the range of the parameters of the system in which nonlinear effects can manifest themselves.

It should be noted that, in the considered model, the possibility of rapid decaying of the third level was initially assumed, as a consequence of which population of this level ρ_3 should be considerably lower than ρ_2. This circumstance also affects the calculation of multiparticle contributions. Therefore, it is useful to know the range of the parameters of the system in which this condition is fulfilled. For this reason, we plotted curves *3* in Fig. 7, which successively (from left to right) correspond to the ratios $\rho_3/\rho_2 = 0.1$, 0.2, and 0.3.

At a higher magnification, these curves, including the curve for $\rho_3/\rho_2 = 0.01$, are shown in Fig. 8. All these curves were plotted such that the ratio of ρ_3 to ρ_2 (as a function of $\bar{\Omega}$) is maximal. Consequently, at specified values of parameters α and $\bar{\Delta}$, on the chosen curve, all other values of the ratio ρ_3/ρ_2, that correspond to these parameters will be only smaller. It can be easily seen that, with decreasing ratio, corresponding curves are shifted to the left to the $\bar{\Delta}$ axis.

Figure 9a shows the dependence of ρ_2 on α on the boundaries of the range of existence of hysteresis. Here, the dashed curve corresponds to the case in which multiparticle contributions are not taken into account, while the solid curve corresponds to involving these contributions into consideration. It is seen that, when multiparticle contributions are taken into account, ρ_2 increases with increasing α considerably more rapidly and, at a shorter base, reaches considerably higher values than in the opposite case. In Fig. 9b, on the same boundaries and by the same curves, we plotted the dependences of the ratio ρ_3/ρ_2 on α. In this figure, the range of only rather small values of this ratio is shown. It is also seen that the solid curve goes steeper than the dashed curve; however, at small values of ρ_3/ρ_2, the difference between the two dependences is not so significant as in Fig. 9a.

Therefore, taking into account three-particle interference contributions in the equations of motion leads to a restriction of the range of existence of hysteresis. However, at the same time, taking into account these contributions makes it possible to more reliably single out the range of parameters in which essentially nonlinear effects can manifest themselves. This, in

turn, narrows the range of searching for real physical systems that correspond to the required parameters.

ACKNOWLEDGMENTS

This work was supported by a grant from the St. Petersburg National Research University of Information Technologies, Mechanics, and Optics; by a Russian–Israeli grant for nanotechnology (no. 3-5803); by a grant from the Russian Foundation for Basic Research (13-02-00527); and by the program of the Russian Academy of Sciences "Basic Problems of Nonlinear Dynamics in Mathematical and Physical Sciences."

REFERENCES

1. V. A. Malyshev, H. Glaeske, and K. H. Feller, Phys. Rev. A: **58** (1), 670 (1998).
2. V. A. Malyshev and P. Moreno, Phys. Rev. A: **53** (1), 416 (1996).
3. V. Malyshev, H. Glaeske, and K. Feller, Phys. Rev. A: **65** (3), 033821 (2002).
4. J. A. Klugkist, V. Malyshev, and J. Knoester, J. Chem. Phys. **127** (16), 164705 (2007).
5. J. A. Klugkist, V. Malyshev, and J. Knoester, J. Chem. Phys. **128** (8), 084706 (2008).
6. N. V. Vysotina, V. A. Malyshev, V. G. Maslov, L. A. Nesterov, N. N. Rosanov, S. V. Fedorov, and A. N. Shatsev, Opt. Spektrosk. **109** (1), 1185 (2010).
7. B. N. Levinskii, L. A. Nesterov, B. D. Fainberg, and N. N. Rosanov, Opt. Spektrosk. **115** (3), 464 (2013).

Translated by V. Rogovoi